MULTIFUNCTIONAL FUSION RAMAN SPECTROMETER FOR THE DETECTION OF CONTROLLED HAZARDOUS LIQUIDS

F. Hao*, Q. Zhang, Ch. Jin, T. Zhang, E. Jia, H. Yu, Zh. Fan, F. Du

First Research Institute of the Ministry of Public Security, Beijing 100048, China; e-mail: haofenglong110@126.com

There have been severe challenges in the security inspection of controlled hazardous liquids in public places in recent years. To further meet the practical requirements of the front line of security inspection, we designed and developed a hazardous liquid detector on the basis of the fusion of Raman spectroscopy, dielectric constant, and heat conduction. The design ideas and methods for the whole system, as well as its hardware and software platforms, are expounded emphatically. Several inflammable and explosive hazardous liquids, including gasoline, methanol, acetonitrile, and toluene, as well as water, were selected as samples and sealed in transparent and opaque containers to test the performance of the instrument. As shown by the experimental results, the three subsystems can quickly and non-destructively detect the corresponding samples without false positives or false negatives. The instrument has various detection functions that overcome the single technical defects and has broad application prospects.

Keywords: *security inspection, hazardous liquids, Raman spectroscopy, dielectric constant, heat conduction.*

МНОГОФУНКЦИОНАЛЬНЫЙ КР-СПЕКТРОМЕТР ДЛЯ ОБНАРУЖЕНИЯ ПОТЕНЦИАЛЬНО ОПАСНЫХ ЖИДКОСТЕЙ

F. Hao*, Q. Zhang, Ch. Jin, T. Zhang, E. Jia, H. Yu, Zh. Fan, F. Du

УДК 535.375.5:66.06

Первый научно-исследовательский институт Министерства общественной безопасности, Пекин 100048, Китай; e-mail: haofenglong110@126.com

(Поступила 14 мая 2020)

Разработан детектор потенциально опасных жидкостей на основе сочетания спектроскопии комбинационного рассеяния, диэлектрической проницаемости и теплопроводности. В качестве образцов отобраны легковоспламеняющиеся и взрывоопасные жидкости (бензин, метанол, ацетонитрил и толуол), а также вода и запечатаны в прозрачные и непрозрачные контейнеры для проверки работоспособности прибора. Показано, что три подсистемы могут быстро и неразрушающим образом обнаруживать соответствующие образцы без ложных срабатываний. Прибор имеет различные функции обнаружения, позволяющие преодолеть отдельные технические дефекты, и перспективен для широкого применения.

Ключевые слова: *проверка безопасности, опасные жидкости, спектроскопия комбинационного рассеяния, диэлектрическая постоянная (проницаемость), теплопроводность.*

Introduction. The rampant explosion of terrorist activities in the 21st century constitutes a serious challenge to the security of public places, posing a great threat to people's lives and properties [1]. Worldwide, relevant laws and regulations to enhance safety inspection standards at airports, customs checkpoints, railway stations, passenger stations, subway stations, and other public transport hubs and major public spaces have been promulgated. In recent years, cases of terrorist attacks or revenge against the society have been perpetuated from time to time using hazardous goods [2, 3]. Some explosions were carried out using hazardous chemicals and inflammable and explosive materials. However, controlled hazardous liquids are difficult to quickly and effectively detect through commonly used security inspection equipment. Liquid goods remain restricted in airports. The conventional methods for identifying such liquids at train stations involve opening the bottles and trying to drink them. However, comprehensive detection equipment remains insufficient in subway stations and other public places, which poses serious security risks. Most existing detection equipment are based on a single technology, such as Raman spectroscopy, dielectric constant, and heat conduction, which cannot satisfy all the requirements of security inspection.

The basis of Raman spectroscopy is the Raman effect that was first observed by the Indian scientist, Raman, in 1928. When light is scattered from a molecule, most photons are elastically scattered. The scattered photons have the same energy (frequency) and, therefore, wavelength, as the incident photons. However, a small fraction of light is scattered at optical frequencies different from and usually lower than the frequency of the incident photons. The process that leads to this inelastic scattering is termed the Raman effect. Raman scattering can occur with a change in the vibrational, rotational, or electronic energy of a molecule. The Raman scattering effect is closely related to the molecular structure and is a fingerprint spectrum that can characterize the molecular structure of materials [4–7]. Figure 1 shows the energy level diagram for Raman scattering. E_0 and E_1 represent the ground and vibrational excited states, respectively. It is assumed that the laser frequency acting on the sample is ν_0, and the corresponding photon energy is $h\nu_0$.

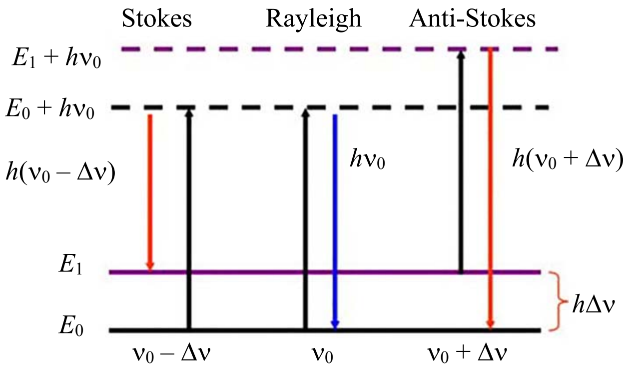

Fig. 1. Energy level diagram for Raman scattering.

When a molecule is excited by incident light from its ground state, E_0 (or vibrational excited state E_1), it moves to a virtual state with energy level $E_0 + h\nu_0$ (or $E_1 + h\nu_0$) and then decays back to the ground state, E_0 (or vibrational excited state E_1). This scattering phenomenon is called Rayleigh scattering. The other scattering process is inelastic, whereby the photon energy of the scattered light is different from that of the incident light. This process has two results: one is that a molecule in the ground state is excited to the virtual state by the incident light with energy, $h\nu_0$, after which it decays to the vibrational excited state E_1. This type of Raman scattering is called the Stokes scattering and is usually observed in Raman spectroscopy, and the corresponding energy is $h(\nu_0 - \Delta\nu)$. The other is called the anti-Stokes scattering, and the corresponding energy is $h(\nu_0 + \Delta\nu)$. The abscissa of the Raman spectra represents the Raman shift, $\Delta\nu$ ($\Delta\nu = \nu_0 - \nu_{\text{scattered}} = \pm\nu_s$). $\Delta\nu$ is a physical quantity that characterizes the vibrational and rotational levels of molecules. It is the basis of quantitative structural analysis. Different samples possess different $\Delta\nu$s. $\Delta\nu$ is generally represented by the reciprocal of the wavelength and has a unit of cm^{-1}. Currently, detection instruments based on Raman spectroscopy are widely used in security inspection [8], to suppress customs smuggling [9], drug control [10], forensic identification [11], in situ analysis, and so forth [12, 13].

The dielectric constant is a physical quantity that characterizes the ability of a material to store charges in an electric field [14]. Different liquids have different dielectric constants [15]. It can be used to determine if a liquid is hazardous because the dielectric constant can show what type of liquid a test sample is. From the principles of electrostatics, an electric field, E, is generated around an isolated charge, q, in vacuum. If another charge, q_0, enters the electric field and is affected by the electric field force, then the electric field intensity generated by the charge q can be expressed as

$$\mathbf{E} = \frac{q}{4\pi\varepsilon_0 r^2}\mathbf{r} \ , \tag{1}$$

where ε_0 is the dielectric constant of vacuum and r is the radius of q. The field intensity generated by the charge q_0 in non-vacuum media is given by

$$\mathbf{E} = \frac{q}{4\pi\varepsilon r^2}\mathbf{r} \ , \tag{2}$$

where ε is the dielectric constant of the material ($\varepsilon_0 = 8.854187817\times10^{-12}$ F/m is generally taken as the reference standard for the dielectric constant of vacuum). The ratio of ε to ε_0 is defined as the relative dielectric constant, ε_r:

$$\varepsilon_r = \varepsilon/\varepsilon_0 \geq 1 \ . \tag{3}$$

Although vacuum is an ideal dielectric model, there is no vacuum in test environments; therefore, the relative dielectric constant, ε_r, of the measured liquid is always greater than or equal to 1.

Thermal conductivity is a parameter used to characterize the thermal conductive properties of a substance. It is evaluated as follows: taking two parallel planes with an area of 1 m^2 in a direction perpendicular to the internal heat conduction of an object, the distance between the two planes should be ensured to be 1 m. If the temperature difference between the two parallel planes is 1 K, then the heat transferred from the plane at a higher temperature to the plane at a lower temperature in 1 s is defined as the thermal conductivity of the substance, with units in $W\cdot m^{-1}\cdot K^{-1}$. If there is no heat loss, the thermal conductivity of block objects with opposite sides parallel to each other can be derived as

$$\lambda \mathrm{A}\left(\theta_2 - \theta_1\right)/1 = E/t \ , \tag{4}$$

where λ is the thermal conductivity, A is the cross-sectional area of the parallel planes, θ_2 and θ_1 are the temperatures of the two planes, and l is the distance between the two planes. The derivative of Eq. (4) can be expressed as

$$\lambda \mathrm{A} d\theta / dl = dE / dt \ . \tag{5}$$

Objects with high thermal conductivities are referred to as excellent thermal conductors, whereas those with low thermal conductivities are referred to as thermal insulators or poor thermal conductors. Thermal conductivity is affected by temperature, depending on some conditions. That is, the thermal conductivity of an object λ increases slightly within a range as the temperature of the object increases. Hence, if the difference in temperature between the interiors of an object is small, the thermal conductivity λ is usually regarded as constant. Liquids with different properties have different thermal conductivities. Different liquids have different temperature responses to the same heating conditions and heating duration. Therefore, their thermal conductivities can be calculated using the difference in their temperature. Conversely, the properties of liquids can be distinguished using their thermal conductivities [16].

Table 1 shows the dielectric constant and thermal conductivity of some liquids at 20°C. For instance, the dielectric constant of water is 80.2, and the thermal conductivity is 0.60. The dielectric constant and thermal conductivity of hazardous liquids are relatively small. Therefore, the dielectric constant and thermal conductivity can be used to determine whether or not a liquid is hazardous.

Ramirez et al. showed that Raman spectroscopy can be used to accurately detect the chemical composition of hazardous liquids in transparent containers [17]. They detected hazardous liquids concealed in glass and plastic containers. However, they could not detect hazardous liquids in opaque containers such as ceramics, soft packaging, and metal. Janezic et al. investigated the feasibility of using the dielectric constant to classify hazardous and nonhazardous liquids [18]. However, qualitative detection cannot be achieved using this technology. Using three different experimental methods, Kwon et al. introduced and developed a validation chain for measuring the thermal conductivity of liquids [19]. Ziouche et al. proposed a technique for measuring thermal conductivity using a temperature sensor and a heater with an integrated sharp tip [20]. Qualitative detection cannot be realized through heat conduction technology alone, which is limited to the detection of liquids in metal containers. Hence, we designed and developed a hazardous liquids detector on the basis of the fusion of Raman spectroscopy, dielectric constant, and heat conduction to address the above problems. The instrument can overcome the limitations of using a single technology and has a variety of detection functions. Table 2 shows the comparison of the containers that can be detected by various technologies. The multifunctional fusion detector can simultaneously detect hazardous liquids in transparent and opaque containers such as plastics, glass, ceramics, and metals and further satisfy the practical needs of public places.

TABLE 1. Dielectric Constant and Thermal Conductivity of Some Liquids

Substance name	Dielectric constant	Thermal conductivity, $W \cdot m^{-1} \cdot K^{-1}$
Water	80.2	0.60
Formic acid	58.5	0.27
Ethylene glycol	37.7	0.26
Acetonitrile	36.6	0.19
Nitrobenzene	36.4	0.14
Methanol	32.6	0.20
Ethanol	24.3	0.17
Acetone	20.7	0.16
1-Hexanol	13.3	0.15
Ethyl acetate	6.0	0.14
Carbon disulfide	2.6	0.14
Toluene	2.4	0.13
Benzene	2.3	0.14
Carbon tetrachloride	2.2	0.10
Gasoline	1.9	0.11

TABLE 2. Comparison of Detectable Containers between Different Technologies

Technology / Container material	Raman spectroscopy	Dielectric constant	Heat conduction	Multifunctional fusion
Plastic	Yes	Yes	No	Yes
Glass	Yes	Yes	No	Yes
Ceramics	No	Yes	No	Yes
Metal	No	No	Yes	Yes

Materials and methods. The multifunctional fusion detector combines Raman spectroscopy, dielectric constant, and heat conduction technology. It has multiple detection functions and overcomes the defects of using a single technology. It is especially suitable for the detection of hazardous liquids in public places. The development of the instrument is of great significance for curbing the occurrence of terrorist activities and maintaining social harmony and stability. The design comprises three parts: whole system design, hardware platform design, and software platform design.

Whole system design. The whole system design takes performance, stability, detection time, and scalability as design objectives. It allocates functions to users and instruments reasonably to achieve the best matching for the system. The multifunctional fusion detector comprises four parts: Raman spectroscopy subsystem, dielectric constant subsystem, heat conduction subsystem, and control and display system. The Raman spectroscopy subsystem design is based on chromatic dispersion. Compared with the Fourier transform type, it has the advantages of compact structure, high detection speed, and high sensitivity. This subsystem can be used to detect, accurately name, and categorize hazardous liquids in transparent and translucent containers. The dielectric constant subsystem is responsible for the detection of hazardous liquids in nonmetal containers such as ceramics, plastics, and opaque glass. The heat conduction subsystem is responsible for the detection of hazardous liquids in metal containers. The control and display subsystem is responsible for the overall operational control, function realization, and results display.

Hardware platform design. We designed the hardware platform on the basis of dual CPU in accordance with the design requirements of the system and the use requirements of airports, customs, railway stations, passenger stations, metro stations, and other public spaces. The platform contains a central processor and a data acquisition processor. Figure 2 shows the connection diagram. The central processor is responsible for the operational control of the touch screen, Raman spectroscopy, dielectric constant, and heat conduction subsystems. It is equipped with a USB interface, network interface, power supply lamp, alarm lamp, alarm buzzer, and other functional modules that can realize functions such as data transmission, network connection, power supply, alarm light prompt, and alarm sound prompt.

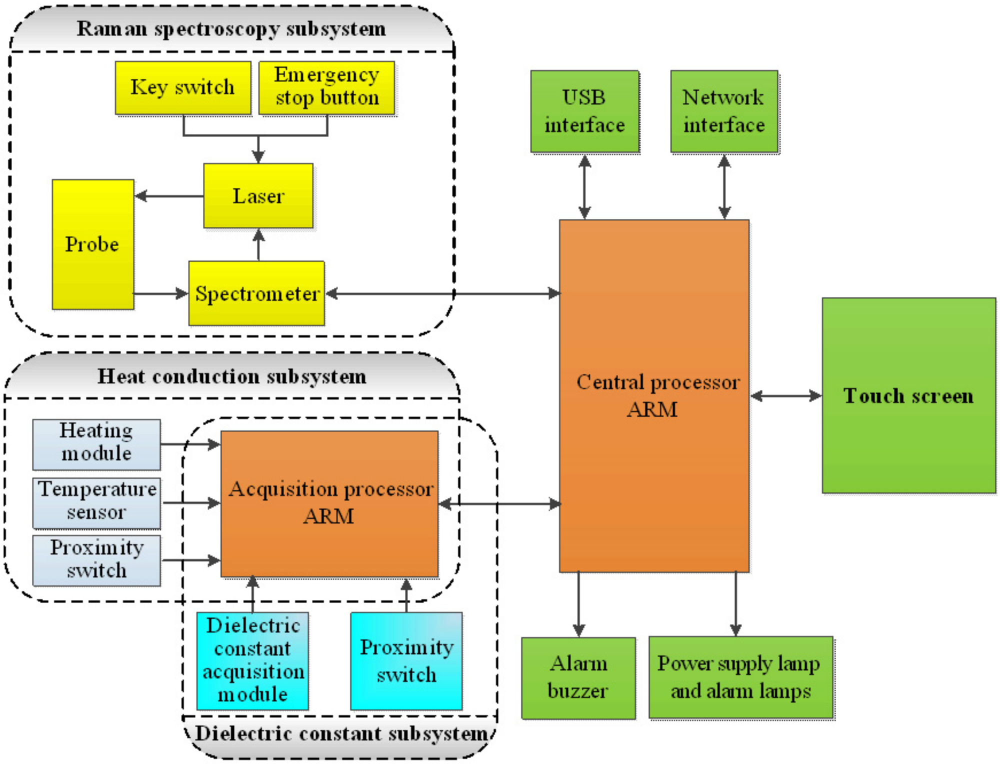

Fig. 2. Composition of the hardware platform.

The Raman spectroscopy subsystem comprises the laser, key switch, emergency stop button, spectrometer, and probe module. The laser is connected via optical fiber to a probe and jointly controlled by a key switch and an emergency stop button. Its main function is to irradiate a sample and produce the Raman scattering effect. The spectrometer is connected via optical fiber to a probe, and its main function is to collect Raman spectroscopy signal. The dielectric constant subsystem comprises a proximity switch, a dielectric constant acquisition module, and an acquisition processor. The proximity switch function determines the proximity of the detected sample and starts the subsystem. The acquisition module collects the dielectric constant of the liquid in nonmetal containers, and the acquisition processor collects and processes the data returned by the acquisition module. The heat conduction subsystem comprises the proximity switch, heating module, temperature sensor, and acquisition processor. The proximity switch determines the proximity of the detected sample and starts the subsystem. The heating module heats liquids in metal containers. The temperature sensor is used to measure temperature changes in the liquid, whereas the acquisition processor is used to collect and process the data returned by the sensor. The dielectric constant subsystem and heat conduction subsystem share an acquisition processor to ensure the stable and efficient operation of the system.

Software platform design. The software platform was designed to support the self-developed detectors, monitor the working status of each module in the hardware platform in real-time, collect Raman signals, and realize human–computer interaction functions. Detectors used in the frontline of anti-terrorism and security inspections must have high real-time stability and operability, thus requiring an embedded operating system. Google's Android operating system is a powerful embedded system that satisfies all the requirements of a multifunctional fusion detector. It is open and scalable and has high user experience [21]. Therefore, we adopted Android as the embedded operating system for the detector and used the Android Studio as the development environment to realize human–computer interaction on the software platform. The software platform is divided into four functional modules based on the system composition, working principle, and functional requirements of the detector: Raman spectroscopy, dielectric constant, heat conduction, and system setting.

The Raman spectroscopy, dielectric constant, and heat conduction modules are divided into three submodules, namely, sample detection, history record, and parameter setting. The sample detection sub-module realizes the core functions of each system and is responsible for detection and results display. Each sample detection sub-module operates independently and simultaneously. The history record sub-module is responsible for the preservation and inspection of historical data. When hazardous liquids are detected, the software system automatically saves the detected data to the history record module, thereby improving the efficiency of the instrument. The parameter setting sub-module is responsible for setting the detection parameters of the corresponding subsystems. The system setting module sets the function for the whole system, and it is the basic module for setting the parameters and viewing auxiliary functions in the instrument. This module is divided into five sub-modules, namely, account management, communication module, general settings, transmission interface, and software version.

Sample detection process. The three subsystems operate independently and simultaneously without interference. Figures 3 depicts the sample detection process. Detection is performed by selecting the corresponding subsystems based on the material in a sample container. The detection results for each subsystem are displayed in the corresponding area of the software platform after detection is completed, and recommendations are given whether to pass the sample or not. If hazardous liquids are detected, the buzzer will sound an alarm and the alarm lamp will flash simultaneously.

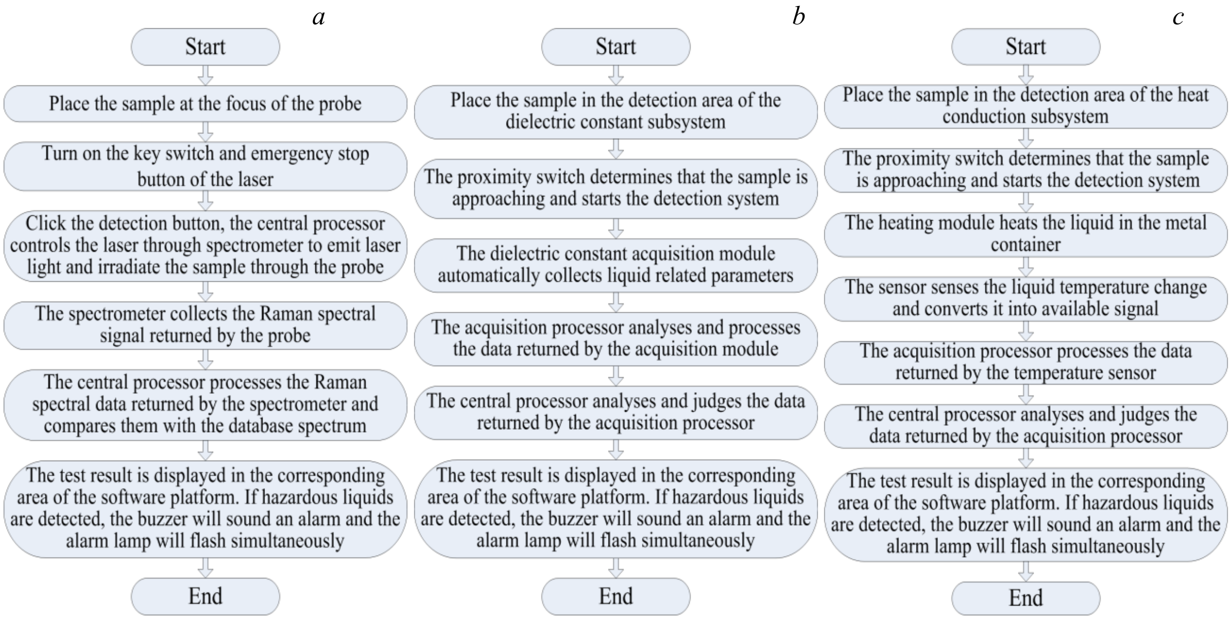

Fig. 3. Sample detection process. (a) Raman spectroscopy subsystem, (b) dielectric constant subsystem, and (c) heat conduction subsystem.

Results and discussion. We selected four inflammable and explosive hazardous liquids, namely, gasoline, methanol, acetonitrile, and toluene, as well as water, as test samples in order to test the performance of the multifunctional fusion detector. The octane number of gasoline is 95, the other three hazardous liquids were analytically pure, and water was pure. At room temperature, five kinds of substances were sealed separately in corresponding containers. Table 3 shows the specific detection conditions and results.

The samples in transparent glass bottles were detected via the Raman spectroscopy subsystem, those in the ceramic bottles were detected through the dielectric constant subsystem, whereas the samples in aluminum cans were detected via the heat conduction subsystem. The detection time and alarm results were recorded. The detection times were recorded by an experimenter, and the results were recorded to seconds accuracy.

As indicated in Table 3, the three subsystems can quickly and non-destructively detect the corresponding samples. The detection time for the five samples in the Raman spectroscopy subsystem is less than 5 s, whereas the detection speed is high. According to the Raman principle, this subsystem can realize qualitative detection. As shown in Fig. 4, the detection results can reveal the specific name of the sample and the matching coefficient. The abscissa represents the Raman shift, and the ordinate represents relative intensity. We can observe that the Raman characteristic peaks of acetonitrile are clearly distinguishable, with main peak positions at 392.4, 932.6, 1387.7, and 2264.6 cm^{-1}. The signal-to-noise ratio of each peak is very high, with a high matching coefficient of 0.9865.

TABLE 3. Detection Conditions and Results of Five Samples

Subsystem name	Container	Sample name	Sample number	Sample volume (milliliter)	Detection time (second)	Alarm
Raman spectroscopy	Transparent glass sample bottle	Gasoline	RS1#	2	4.41	Yes
		Methanol	RS2#	2	4.45	Yes
		Acetonitrile	RS3#	2	4.44	Yes
		Toluene	RS4#	2	4.39	Yes
		Water	RS5#	2	4.48	No
Dielectric constant	Ceramic bottle	Gasoline	DC1#	100	1.21	Yes
		Methanol	DC2#	100	1.16	Yes
		Acetonitrile	DC3#	100	1.19	Yes
		Toluene	DC4#	100	1.18	Yes
		Water	DC5#	100	1.24	No
Heat conduction	Aluminum can	Gasoline	HC1#	100	4.78	Yes
		Methanol	HC2#	100	4.89	Yes
		Acetonitrile	HC3#	100	4.92	Yes
		Toluene	HC4#	100	4.83	Yes
		Water	HC5#	100	4.96	No

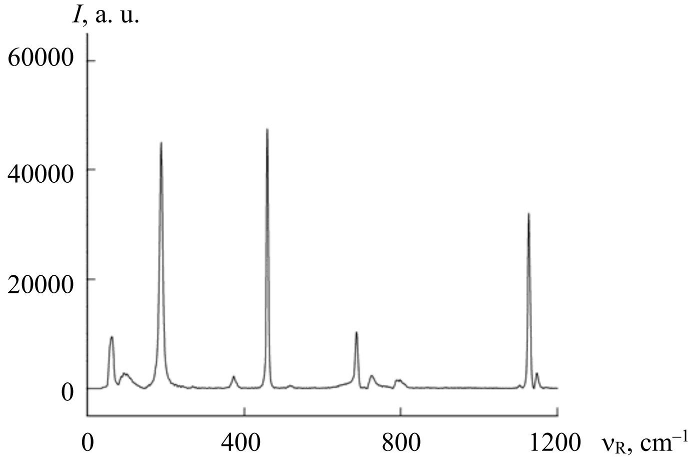

Fig. 4. Detection results for acetonitrile.

The four hazardous liquids all failed the detection test, and alarms were set off. Table 4 shows the detection results. As indicated in Table 4, the main peak positions of each hazardous liquid are all clearly distinguishable, and the matching coefficient is relatively high.

The experimental results show that the characteristic peaks of the four hazardous liquids are consistent with that of the standard, and the matching coefficients were all higher than 95%, which further proves the accuracy of the detection of the Raman spectroscopy subsystem.

TABLE 4. Detection Results of Four Hazardous Liquids

Sample name	Main peak positions, cm^{-1}	Matching coefficient
Gasoline	1313.8, 1457.4	0.9568
Methanol	1048.2, 1464.5	0.9625
Acetonitrile	392.4, 932.6, 1387.7, 2264.6	0.9865
Toluene	534.7, 798.5, 1016.4, 1222.6	0.9733

According to the dielectric constant principle and heat conduction principle, these two subsystems can determine whether the samples are hazardous liquids and show the information of whether they pass. Table 3 shows that the dielectric constant subsystem has high detection speed, and the detection time for the samples is less than 2 s. Four hazardous liquids all failed the detection test, and alarms were set off. The detection time for samples in the heat conduction subsystem is less than 5 s, and the speed meets the requirements for security inspection. Hazardous liquids all failed the detection test, and alarms were set off. However, water passed the detection test.

At the same time, to verify the detection performance of Raman spectroscopy subsystem for liquids with different concentrations, 100% acetone, 70% acetone (30% ethanol as the solvent), and 30% acetone (70% ethanol as the solvent) solutions were selected as samples. Figure 5 shows the detection results of 100% acetone. We can observe that the Raman shift of acetone at different concentrations, namely, 489, 528, 786, 1066, 1222, 1430, and 1710 cm^{-1}, is unchanged, which is basically consistent with the values in reference [22]. The peak intensity decreases with the decreasing of the concentration, and it is still clearly discernable. The result shows that the Raman spectroscopy subsystem can accurately detect liquids with different concentrations.

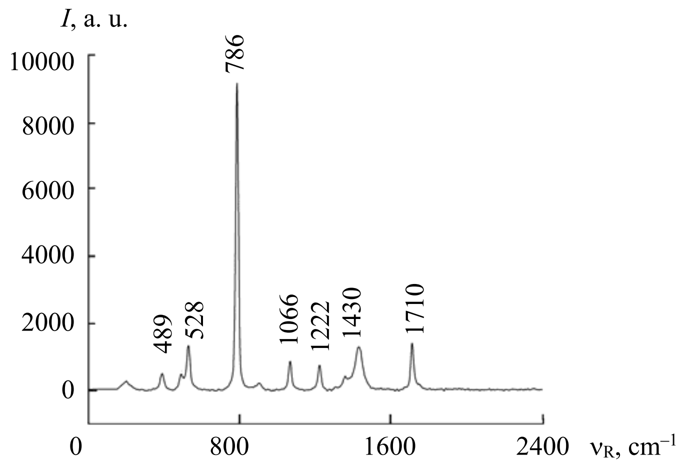

Fig. 5. Detection results for acetone.

We conducted 50 repeated tests on gasoline using the three subsystems, to further verify the testing stability as well as false negatives and false positives of the detector. The experimental results show that the detection time for the Raman spectroscopy subsystem is less than 5 s, that of the dielectric constant subsystem is less than 2 s, and that of the heat conduction subsystem is less than 5 s. No false negatives and false positives were recorded, indicating that the instrument has high stability and high detection accuracy. The detector satisfies the requirements of detectors for anti-terrorism and security inspection. However, there are still some shortcomings in this study. For example, the Raman database is imperfect, and the effect of container size and wall thickness on the detection results has not been studied.

Conclusions. We have successfully designed and developed a multifunctional fusion detector that can solve the problem of simultaneously detecting hazardous liquids in transparent and opaque containers such as plastics, glass, ceramics, and metals. The experimental results demonstrated that the detector has no false positives or false negatives, and the Raman matching coefficients are higher than 95%. In the future, we will supplement the database of hazardous liquids, study the effect of container size and wall thickness on the results, and attempt to further reduce the detection time. The market competitiveness of the product will also be constantly enhanced.

Acknowledgments. This work was supported financially by the Central Public-Interest Scientific Institution Basal Research Fund of China (No. A18611GY).

REFERENCES

1. R. Golan, D. Soffer, A. Givon, I. T. Group, K. Peleg, *Injury,* **45**, No. 1, 39–43 (2014).
2. A. V. Shvetsov, S. V. Shvetsova, *Eur. J. Security Res.*, **2**, No. 2, 131–145 (2017).
3. B. Hoffman, F. Reinares, *The Evolution of the Global Terrorist Threat: from 9/11 to Osama bin Laden's Death*, Columbia University Press, New York (2014).
4. M. L. Ramírez, W. Ortiz, L. C. Pacheco, S. P. Hernández, *IEEE. Sensors J.,* **10**, No. 3, 693–698 (2010).
5. W. E. Smith, G. Dent, *Modern Raman Spectroscopy – a Practical Approach*, John Wiley & Sons Ltd., Chichester (2005).
6. S. G. Cho, J. H. Chung, *SPIE Defense, Security, & Sensing*, **87210U**, 1–6 (2013).
7. X. L. Liu, H. N. Liu, P. H. Tan, *Rev. Sci. Instrum.*, **88**, No. 8, 1–5 (2017).
8. B. Cletus, W. Olds, P. M. Fredericks, E. Jaatinen, E. L. Izake, *J. Forensic Sci.*, **58**, No. 4, 1008–1014 (2013).
9. S. Almaviva, S. Botti, A. Palucci, A. Puiu, F. Schnürer, W. Schweikert, F. S. Romolo, *Opt. Eng.*, **53**, No. 4, 1–8 (2014).
10. G. S. Bumbrah, R. M. Sharma, *Egypt. J. Forensic Sci.*, **6**, No. 3, 209–215 (2016).
11. S. R. Khandasammy, M. A. Fikiet, E. Mistek, Y. Ahmed, L. Halámková, J. Bueno, I. K. Lednev, *Forensic Chem.*, **8**, 111–113 (2018).
12. M. Guerra, S. Longelin, S. Pessanha, M. Manso, M. L. Carvalho, *Rev. Sci. Instrum.,* **85**, No. 6, 1–9 (2014).
13. H. B. Li, W. H. Luo, G. Li, G. F. Zhang, P. C. Zhang, C. M. Li, Y. J. Gu, *Rev. Sci. Instrum.,* **89**, No. 8, 1–5 (2018).
14. Y. Nogi, M. Watanabe, K. Suzuki, *Am. J. Phys.*, **83**, No. 9, 782–786 (2015).
15. M. Karami, P. Rezaei, S. Kiani, R. A. Sadeghzadeh, *Electron. Lett.*, **53**, No. 19, 1300–1302 (2017).
16. M. L. Ramirez, W. Ortiz, O. Ruiz, L. Pacheco, S. P. Hernández, *Proc. SPIE – The Int. Soc. Opt. Eng.*, **6538**, 1–9 (2007).
17. M. L. Ramirez, N. Gaensbauer, H. Felix, W. Ortiz, L. Pacheco, S. P. Hernández, *Int. J. Spectrosc.,* **2012**, 1–7 (2012).
18. M. D. Janezic, J. D. Splett, K. J. Coakley, *J. Res. Natl. Inst. Stand. Technol.*, **119**, No. 3, 256–271 (2014).
19. S. Kwon, J. Lee, D. H. Kim, *J. Kor. Phys. Soc.*, **68**, No. 10, 1145–1155 (2016).
20. K. Ziouche, Z. Bougrioua, P. Lejeune, T. Lasri, D. Leclercq, *Measur. Sci. Technol.*, **26**, No. 8, 1–8 (2015).
21. S. B. Almin, M. A. Chatterjee, *Proc. Comput. Sci.*, **45**, 407–417 (2015).
22. P. Mohapatra, S. Panigrahi, *J. Food Res.*, **1**, No. 1, 3–12 (2012).